Oxygen-deficient centers and excess Si in buried oxide using photoluminescence spectroscopy

Hiroyuki Nishikawa
Department of Electrical Engineering, Tokyo Metropolitan University, 1-1 Minami-Osawa, Hachioji, Tokyo 192-0397, Japan

Robert E. Stahlbush
Naval Research Laboratory, 4555 Overlook Avenue, Washington, D.C. 20375-5320

James H. Stathis
IBM T. J. Watson Research Center, P.O. Box 218, Route 134, Yorktown Heights, New York 10598

(Received 9 June 1999)

Defects in buried oxide (BOX) in Si prepared from the separation by implantation of oxygen (SIMOX) technique under various preparation conditions such as doses of oxygen [$(0.39-1.9)\times10^{18}\,\mathrm{cm}^{-2}$] and anneal temperatures (1310–1350 °C) were investigated by a photoluminescence technique using synchrotron radiation as a light source. Under excitation at 5.0 eV at room temperature, all the SIMOX BOX samples typically exhibit a broad photoluminescence (PL) band in the range of 2–3 eV, which can be deconvoluted into three Gaussian components at 3.1, 2.6–2.8, and 2.4 eV. The 3.1- and 2.6–2.8-eV bands have lifetimes of about 2–45 ns, while the 2.4-eV band has a much longer lifetime. In addition, some high-dose SIMOX BOX's prepared with multiple oxygen implant steps show a 4.4-eV PL band with a lifetime of about 4 ns associated with a form of oxygen-deficient centers (ODC's) called ODC(II) in a-SiO_2, which were suppressed by a supplemental oxygen implantation. The behavior of the short-lived 2–3-eV PL components was sensitive to the oxygen doses and anneal temperatures, and conditions that tended to increase the 2–3-eV PL tended to decrease the 4.4-eV band. Etchback experiments of the BOX layer show that the defects responsible for the 2–3-eV band were located at the BOX close to the superficial Si/BOX interface, while those for the 4.4-eV band exist throughout the whole BOX layer. Comparison with high-temperature oxide grown on Si at 1350 °C suggests that the postimplantation, high-temperature anneal results in the generation of defects responsible for the short-lived 2–3-eV bands. Based on the similarities with the PL bands in Si clusters in SiO_2, we conclude that the 2–3-eV bands in the BOX's are associated with Si clusters in SiO_2. [S0163-1829(99)03247-6]

I. INTRODUCTION

The buried oxide (BOX) prepared from the separation by implantation of oxygen (SIMOX) technique is one of the key materials for the realization of silicon-on-insulator (SOI) technologies. However, the SIMOX BOX exhibits peculiar properties due to differences both in structural and electrical properties,[1] when compared with conventional thermal oxide on Si. Electrically active defects in the BOX of the SIMOX wafers, or other SiO_2 films, have been studied mostly with electrical (charge-sensing) techniques and with electron spin resonance (ESR). The electrical studies have typically shown that the BOX of the SIMOX has a much higher concentration of electron and hole traps than normal thermal oxide,[2,3] and higher concentration of the E' centers are observed by ESR measurements in SIMOX than in thermal oxide.[4] These studies concluded that during the postimplantation, high-temperature (>1300 °C) anneal that is necessary to form the SIMOX BOX, defects such as oxygen vacancies are generated. The distinctive properties of the buried SiO_2 network have also been demonstrated by the presence of Si clusters.[3,5,6] Thus, apart from the technological importance, the formation of defects in the BOX's and their peculiar properties are quite interesting from a basic physics viewpoint.

Among these studies, successful studies on oxygen-deficient centers (ODC's) in the SIMOX BOX have been made using a photoluminescence (PL) technique under excitation by synchrotron radiation.[7] The concentration of the ODC's in the SIMOX BOX was estimated to be as high as $\sim10^{20}\,\mathrm{cm}^{-3}$.[8] This concentration is consistent with electrical studies of electron traps,[9] which theoretical studies have indicated are due to oxygen vacancies.[10] Thus, the PL measurement, which is a complementary technique to electrical and ESR measurements, can give new insights into the defects in SiO_2. The usefulness of the technique has been demonstrated by a series of PL studies on various forms of a-SiO_2, including bulk silica[11] and damaged thermal oxide.[12]

In this paper, we report the results of a PL study on the SIMOX BOX's prepared under various conditions such as oxygen doses and annealing temperatures. The formation of these PL centers is highly sensitive to manufacturing conditions such as oxygen doses and annealing temperatures. The PL bands in the 2–3-eV range are attributed to Si clusters and provide a method for studying how the SIMOX fabrication conditions affect Si cluster formation.

II. EXPERIMENT

Samples used in the present experiments were BOX layers produced by the SIMOX technique. Samples include low-dose [$(0.39-0.6)\times10^{18}\,\mathrm{cm}^{-2}$] single-implant (SI) BOX's, intermediate-dose ($0.9\times10^{18}\,\mathrm{cm}^{-2}$) double-implant

TABLE I. Sample list.

Classification	Anneal temperature in Ar+0.5% O_2 (°C)	Oxygen dose (10^{18} cm^{-2})	BOX thickness (nm)	Implant step[a]	Implant energy and temperature
Low-dose SIMOX	1310, 1330, 1350	0.39–0.53	85–110	SI	200 keV, 590 °C
Intermediate-dose SIMOX	1310	0.9	176	DI	180 keV, 550 °C
High-dose SIMOX	1310 (1000 for supplemental implant)	1.7–1.8	355, 330	SI, TI	200 keV, 570 °C
		1.9	376	TI (1.8×10^{18} cm^{-2}) +Suppl.(0.1×10^{18} cm^{-2})	200 keV, 540 or 640 °C
Reference: High-temperature oxide	1350	None	118		

[a]The SI, DI, TI, and Suppl. represent single, double, triple, and supplemental implantation of oxygen, respectively.

(DI) BOX's, and high-dose [$(1.7-1.8)\times10^{18}$ cm^{-2}], SI and triple-implant (TI) BOX's. The implant energy was 180–200 keV and postimplantation annealing was done in Ar+0.5% O_2 for 5–8 h at various temperatures in the range of 1310–1350 °C. One of the high-dose TI samples received a supplemental oxygen implant at a dose of 0.1×10^{18} cm^{-2}, which was followed by annealing at 1000 °C. The surface Si layer was etched off with hydrazine for the PL measurements on the BOX layer. For reference, a high-temperature thermal oxide grown at 1350 °C in Ar+0.5% O_2 was also investigated. More detailed specifications of these samples are summarized in Table I.

Photoluminescence measurements were carried out[13] using the beamline U9B of the National Synchrotron Light Source (NSLS) facility at Brookhaven National Laboratory (BNL) equipped with an excitation double monochromator (Spex 1680). The PL from the sample was dispersed by a detection monochromator (Chromex) across the 2.5-cm-diam bialkali photocathode of an ITT model no. F4146M position-sensitive detector, which permits simultaneous recording of spectral and temporal characteristics. As otherwise stated, PL excitation was done in air at a wavelength of 248 nm ($h\nu = 5.0$ eV) at room temperature.

III. RESULTS

A. Intermediate- and high-dose SIMOX BOX's

Figure 1 shows the PL spectra of high-dose TI SIMOX BOX's with an oxygen dose of 1.8×10^{18} cm^{-2} with and without a supplemental oxygen implant of 0.1×10^{18} cm^{-2}, under 5-eV excitation and at room temperature. Two PL bands at 4.4 and 2–3 eV were observed for the TI BOX's without a supplemental implantation. After the supplemental implant, the 4.4-eV PL band was suppressed, while the 2–3-eV band was further enhanced. The spectral feature of the enhanced 2–3-eV band is slightly different from that without the supplemental implantation, suggesting that the PL band comprises several components. We note that the 4.4-eV band was only observed for the BOX prepared by multiple oxygen implants, such as the intermediate-dose DI and high-dose TI SIMOX BOX's. It has been often observed that the 4.4-eV PL band is accompanied by a weak PL band at 2.7 eV with a relatively long lifetime of 10 ms.[11,12] It should be cautioned that the 2–3-eV PL band in Fig. 1 was different from the ''long-lived'' 2.7-eV band associated with ODC (II), as shown later.

In order to see the low-energy PL band in detail, we compared the effects of implantation steps on the 2–3-eV band. Shown in Fig. 2 are the PL spectra obtained for BOX's prepared with (a) SI (dose: 1.7×10^{18} cm^{-2}), (b) DI (dose: 0.9×10^{18} cm^{-2}), and (c) TI (dose: 1.8×10^{18} cm^{-2}) implant. Despite the differences in oxygen doses, they exhibit similar broad peaks around 2–3 eV. They can be deconvoluted into three Gaussian peaks at 3.1, 2.7–2.8, and 2.4–2.5 eV. The peak energy slightly varies from sample to sample, depending on the preparation conditions. We noticed

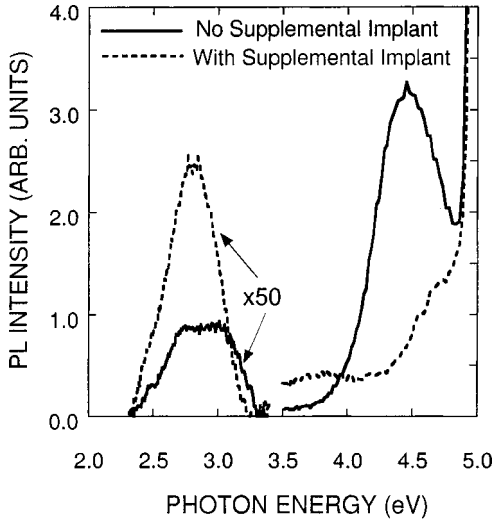

FIG. 1. Typical PL spectra obtained for high-dose triple-implant (dose: 1.8×10^{18} cm^{-2}) SIMOX BOX, with ($t_{ox}=376$ nm) and without ($t_{ox}=355$ nm) supplemental implant (dose: 0.1×10^{18} cm^{-2}).

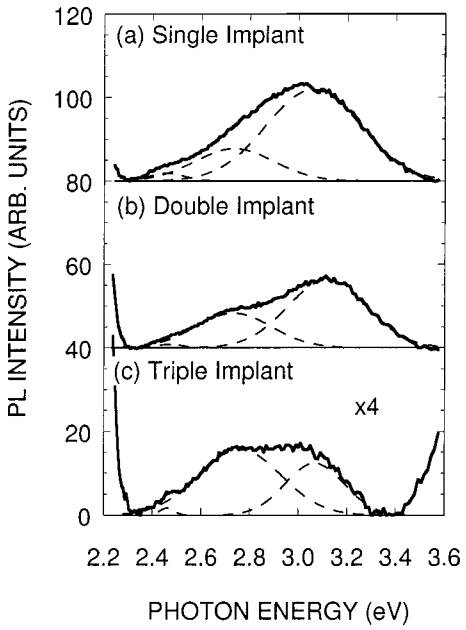

FIG. 2. PL spectra obtained for high-dose SIMOX BOX's for various oxygen doses with different number of implant steps; (a) single implant (dose: $1.7\times10^{18}\,\mathrm{cm}^{-2}$, $t_{ox}=330\,\mathrm{nm}$), (b) double implant (dose: $0.9\times10^{18}\,\mathrm{cm}^{-2}$, $t_{ox}=176\,\mathrm{nm}$) annealed at 1310 °C, and (c) triple implant (dose: $1.8\times10^{18}\,\mathrm{cm}^{-2}$, $t_{ox}=355\,\mathrm{nm}$). Deconvolution was carried out assuming three Gaussian components.

that the 2.4-eV band grows with increasing PL measurement time, suggesting that the 5-eV excitation results in the formation of the PL centers. The formation of the 2–3-eV PL centers strongly depends on the number of implant steps rather than the total oxygen dose. That is, the defects responsible for the 2–3-eV bands decrease with increasing implant steps. The multiple components observed for the 2–3-eV band suggest the presence of several types of defects in the BOX's. In fact, three PL decay components were observed from the time-resolved PL measurements, as shown later. We note again that the 2.7–2.8-eV component is different from the ''long-lived'' 2.7-eV band associated with ODC(II).

Shown in Fig. 3 are the PL decay profiles of (a) the 4.4-eV and (b) the 2–3-eV band for the high-dose TI SIMOX BOX without the supplemental implant, and (c) the 2–3-eV band for the one with the supplemental implant. The decay of the 4.4-eV PL follows approximately a single exponential $[\propto\exp(-t/\tau)]$ with a lifetime of about 4 ns. Based on the peak energy, the PL excitation band at 5 eV, and the lifetime, the 4.4-eV PL can be ascribed to the excited-singlet (S_1) to ground-state (S_0) transition at the site of ODC(II).[11,12] Thus, the supplemental implantation suppressed the generation of the neutral ODC(II) in the TI BOX. Since the oxygen-deficient centers are considered to be one of the major traps in the BOX layers,[1] this is consistent with a previous report[14] showing that SIMOX BOX with a supplemental oxygen has less electron and hole traps.

On the other hand, the 2–3-eV band shows a multiple exponential decay, which was expressed as a sum of several components. As shown in Fig. 3(b), the decay comprises a fast decay with a lifetime of 2.7 ns together with an increased baseline component (by a factor of 10) compared with the one in Fig. 3(a). The increased baseline can be explained by the presence of a very slow ($\tau\sim10\,\mathrm{ms}$) decay component at 2.7 eV due to the triplet-to-singlet transition at the site of the neutral ODC(II).[15] Since the intensity of the ''long-lived'' 2.7-eV component is smaller by an order of magnitude when compared with the short-lived 2–3-eV components as shown in Fig. 3(b), the long-lived component, if any in Figs. 1 and 2, should be buried under the short-lived component. For the TI BOX with supplemental implantation in Fig. 3(c), the fast component with a lifetime of 2.7 ns significantly increases, with an additional decay component with a lifetime of about 18 ns. A very slow component still appears as an increased baseline, which will be later ascribed to the photoinduced PL at 2.4 eV rather than to the long-lived 2.7-eV band.

B. Low-dose SIMOX BOX's and high-temperature thermal oxide

Shown in Fig. 4(a) is a PL spectrum obtained for a low-dose BOX (dose: $0.53\times10^{18}\,\mathrm{cm}^{-2}$, annealed at 1350 °C). Curiously, the 4.4-eV band was not observed for the low-dose BOX's prepared by a single implant step. This is consistent with the preceding observation of the high-dose SIMOX BOX's that the generation of ODC(II) occurs as a result of multiple implant steps. As in the case of the high-dose SIMOX BOX, three Gaussian components can be isolated from the 2–3-eV band. There are two major components at 3.1 and 2.6 eV and a minor one at 2.4 eV. The peak energy varies with oxygen doses by 0.1–0.2 eV as in the case of the high-dose BOX. For comparison, the PL spectrum for high-temperature oxide grown at 1350 °C is also shown in Fig. 4(b). Again, three PL components can be observed almost in the same energy range of 3.1, 2.7, and 2.4 eV for the high-temperature oxide. This indicates that the postimplantation anneal above 1300 °C results in the formation of the 2–3-eV PL centers. It is therefore concluded that the 3.1- and 2.6–2.7-eV bands are due to preexisting defects in the BOX introduced during the high-temperature anneal, while the 2.4-eV band can be ascribed to a photoinduced one. Since the high-temperature oxide does not exhibit the 4.4-eV band, the high-temperature annealing alone does not induce the neutral ODC(II).

Figures 5(a) and 5(b) show the PL decay profiles of the 2–3-eV band for the low-dose SIMOX and the high-temperature oxide, respectively. The low-dose SIMOX shows a fast decay component with a lifetime of about 2.9 ns and a slower one with about 45 ns, together with an increased baseline component. For the case of the high-temperature oxide, three components similar to those for the low-dose SIMOX are observed. Their lifetimes of the two of them are estimated to be 2.3 and 11 ns. The variation in the lifetimes for the fast component from 2.3–2.9 ns and a slower one from 18–45 ns can be accounted for by the differences in the degree of coupling to nonradiative channels affected by the local structure of the defects. Thus, the observed 2–3-eV band is the same as those observed in the high-dose SIMOX BOX's with respect to both the lifetime and the peak energy.

In order to obtain information on the electronic excitation process of the PL band, we measured PL excitation (PLE) spectrum of the 2–3-eV band. Shown in Fig. 6 is a PLE

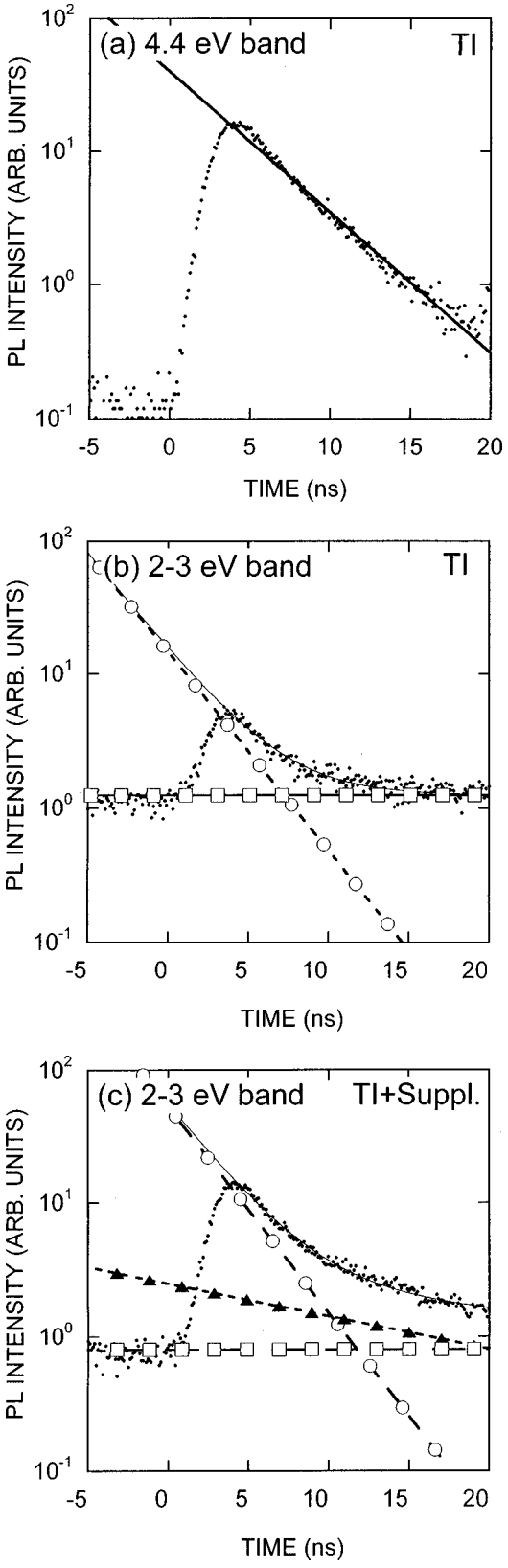

FIG. 3. Decay curves obtained for (a) the 4.4-eV PL band and (b) the 2–3-eV band observed for the triple implant (TI) SIMOX BOX without supplemental implant (○, 2.7 ns) and (c) the 2–3-eV band for the TI BOX with supplemental implant (○, 2.7 ns; ▲, 18 ns). The long-lived 2.7-eV and photoinduced 2.4-eV bands appear as the baseline components, respectively, in (b) and (c) (see text).

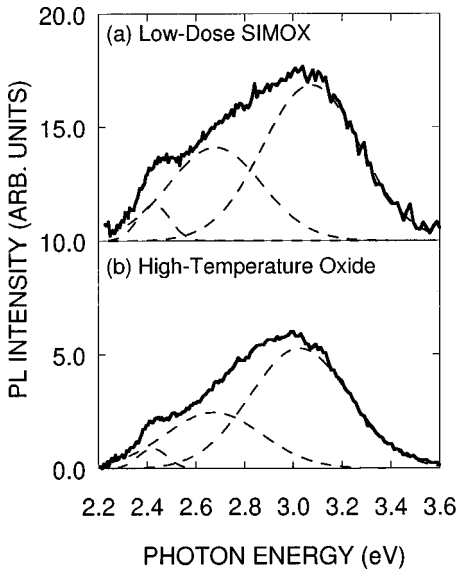

FIG. 4. PL spectra obtained for (a) a low-dose SIMOX (dose: $0.53\times10^{18}\,\mathrm{cm}^{-2}$, annealed at 1350 °C, $t_{ox}=109$ nm) and (b) high-temperature oxide grown on Si in Ar+0.5%O_2 at 1350 °C for 8 h ($t_{ox}=118$ nm). Deconvolution was carried out assuming three Gaussian components.

spectrum obtained for the 2–3-eV band in the low-dose SIMOX BOX. The PLE peak is located at 5.4 eV and exhibits a broad distribution over 4–6 eV. It should be noted that the PLE energy of 4–6 eV coincides with the one at which traps related to excess Si in SIMOX BOX's can be photoionized.[1] This will be discussed in detail in conjunction with the electrical properties of the SIMOX BOX's reported in the literature. We also confirmed that the PLE peak for the 4.4-eV and long-lived 2.7-eV bands in the triple-implant SIMOX lie at 5.0 eV (data not shown). The different energy of the PLE peak is further evidence that ODC(II) is not responsible for the 2–3-eV band. In order to summarize these observations, we show the characteristics of the PL bands for these SIMOX BOX's in Table II.

C. Dependence on oxygen doses and anneal temperatures

Shown in Fig. 7 are the PL intensities as a function of oxygen doses for (a) the low-dose ($<0.53\times10^{18}\,\mathrm{cm}^{-2}$), and (b) the intermediate- and high-dose ($>0.9\times10^{18}\,\mathrm{cm}^{-2}$) SIMOX BOX's. For the low-dose SIMOX BOX's shown in Fig. 7(a), the three PL bands at 3.1, 2.6, and 2.4 eV exhibit similar trends as a function of doses, which have maxima at a dose of $0.49\times10^{18}\,\mathrm{cm}^{-2}$. For the high-dose SIMOX BOX's shown in Fig. 7(b), the intensities of the three PL bands depend on the number of implant steps rather than the oxygen doses (SI>DI>TI). On the other hand, the 4.4-eV PL band associated with ODC(II) increases with the number of implant steps (TI>DI>SI). The latter result indicates that the formation of the 4.4-eV band, or the ODC(II), results from the multiple implant steps, where the damage into BOX layers is expected to occur by the subsequent oxygen implantation into the BOX. In fact, the 4.4-eV PL band has been typically observed in ion-implanted thermal oxide.[12] Thus, the observed 4.4-eV PL band is due to the damage induced by oxygen implantation. Shown in Fig. 8 is the dependence

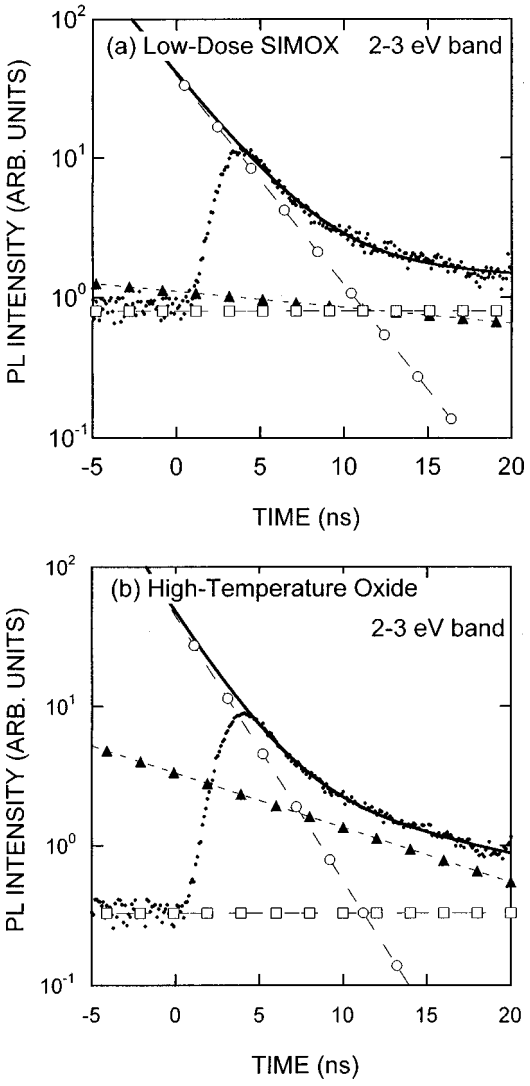

FIG. 5. The PL decay curves of (a) low-dose SIMOX BOX and (b) high-temperature oxide. The lifetimes of these components are (a) ○, 2.9 ns and ▲, 45 ns, and (b) ○, 2.3 ns and ▲, 11 ns. There are additional baseline components (□) due to the photoinduced 2.4-eV bands with longer lifetimes for both samples.

of the PL decay curves on the dose obtained for the low-dose SIMOX. As already seen in Fig. 7(a), the overall intensity of the decay curve shows a maximum at a dose of $0.49\times10^{18}\,\mathrm{cm}^{-2}$. While there is no significant change in the slopes of the fast decay components, the baseline level increases with increasing oxygen doses. The increasing baseline components can be ascribed to the increase of slow decay components with lifetimes longer than the excitation SR pulse interval of 18.9 ns.

The dependence of the PL intensities on anneal temperatures is not straightforward, as shown in Fig. 9. While the behavior differs depending on the oxygen doses, the three PL bands change their intensities in the same manner, suggesting that these PL bands have the same origin. The intensity of the 2–3-eV PL band increases with decreasing anneal temperature for the case of an oxygen dose of $0.51\times10^{18}\,\mathrm{cm}^{-2}$. On the other hand, the intensity showed a maximum at 1330 °C for the case of an oxygen dose of $0.41\times10^{18}\,\mathrm{cm}^{-2}$. These results suggest that the concentration of the 2–3-eV PL center behaves as functions of both anneal temperature and oxygen concentration. Overall, the buried oxide annealed at 1350 °C had the lowest intensity of 2–3-eV PL.

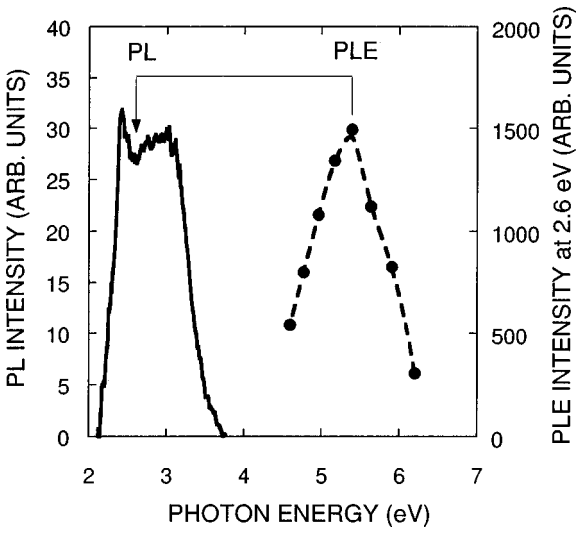

FIG. 6. Photoluminescence excitation spectra of the short-lived 2–3-eV band obtained for a low-dose ($0.49\times10^{18}\,\mathrm{cm}^{-2}$, $t_{ox}=110$ nm) SIMOX BOX annealed at 1310 °C.

D. Depth profile of the PL centers

Shown in Fig. 10 are the PL intensities of the short-lived 2–3-eV band and the 4.4-eV band as a function of HF etch-back time obtained for the low-dose and high-dose SIMOX BOX's. It is shown that the locations of the PL centers are distinctively different between the short-lived 2–3-eV and the 4.4-eV PL bands. While the 4.4-eV PL centers exist throughout the BOX layer, the 2–3-eV PL centers are localized in the BOX close to the top Si/SiO_2 interface.

The increased intensity for the 4.4-eV band after the first etch step in Fig. 10 may be ascribed to the high concentration of defects that will inhibit the penetration of 5-eV photons into the BOX layer. If we assume the removal of about 10% or 40 nm of oxide after the first etch step, the absorption coefficient at 5 eV is estimated to be $2.5\times10^{5}\,\mathrm{cm}^{-1}$, an inverse of the penetration depth of 40 nm. However, this value gives an unreasonably high concentration of the neutral ODC(II) of the order of $\sim10^{22}\,\mathrm{cm}^{-3}$ using a reported oscillator strength of $f=0.15$.[16] If we place an upper limit of $10^{20}\,\mathrm{cm}^{-3}$, which is a reported concentration of ODC(II) in Ref. 8, we obtain the value of $\alpha\sim3\times10^{3}\,\mathrm{cm}^{-1}$, which then gives a penetration depth of $\sim3.7\ \mu$m, much greater than the BOX thickness. Therefore, if there are only ODC(II) defects in the BOX, the PL excitation is deep enough to observe the PL from the whole BOX layer. However, there is another possibility that a high concentration of defects other than ODC(II) can be also present in the BOX close to the top Si/BOX interface. In this case, only the ODC(II)'s within the penetration region of the 5-eV light are observed before the first etching step. We should also take into account the possibility that the PL intensity might have been affected by chemical effects caused by the HF etch. In any cases, we can conclude that the neutral ODC(II)'s exist throughout the whole thickness of the BOX's, though the concentration of

TABLE II. Summary of the PL bands observed for the SIMOX BOX's.

Peak energy (eV)	Decay lifetime	Sample	Origin	Other systems	Electrical properties
4.4, 2.7	4 ns (4.4 eV) 10 ms (2.7 eV)	DI and TI SIMOX BOX	ODC(II): Neutral oxygen vacancy, or twofold coordinated Si (Ref. 16)	Oxygen-deficient-type a-SiO_2, (Ref. 11); ion-implanted thermal oxide (Ref. 12)	Photoinactive traps (Ref. 19)
2–3-eV band (three subpeaks: 3.1, 2.6–2.8, 2.4 eV)	2.3–45 ns, and slow components	All SIMOX BOX and high-temperature oxide	Oxidized Si cluster (Refs. 20–23)	Si^+-implanted thermal oxide (Refs. 20–23)	Photoactive traps (Ref. 19)

defects may be inhomogeneously distributed. These observations are also consistent with the foregoing discussion that the 4.4-eV band is due to ODC(II), a network defect in the BOX's.

The absence of the 2–3-eV PL centers at the BOX/Si substrate side is somewhat puzzling, but might be accounted for either by asymmetry in the generation of the PL centers or by the possibility that the prolonged HF treatment can passivate the PL centers in the bottom Si/SiO_2 interface by hydrogen from the HF solution.

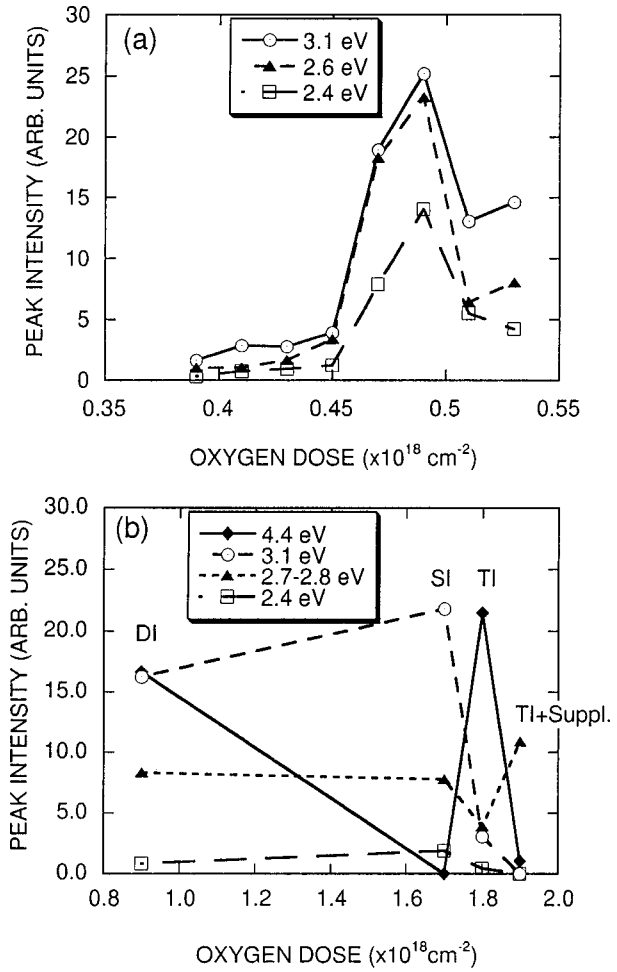

FIG. 7. The intensity of the PL bands as a function of oxygen doses obtained for (a) low-dose ($<0.53\times10^{18}\,cm^{-2}$) and (b) high-dose ($>0.9\times10^{18}\,cm^{-2}$) regions. The SI, DI, TI, and TI+Suppl. in (b) denote single, double, triple implant, and triple implant with supplemental implant, respectively. The 3.1-eV and 2.6–2.7-eV PL bands are short-lived components with lifetimes of about 2–45 ns.

IV. DISCUSSION

A. Excess Si in the SIMOX BOX's

The characteristic feature of the SIMOX BOX is the presence of ODC(II) and excess Si.[1,3] Both the 4.4-eV band with a lifetime of about 4 ns and the long-lived 2.7-eV band can be ascribed to the transitions at the site of neutral ODC(II), as previously reported for oxygen-deficient-type bulk a-SiO_2 (Ref. 11) and damaged thermal oxide (Ref. 12). On the other hand, the short-lived 2–3-eV band has, to our knowledge, never been reported for any types of thermal or buried SiO_2. Since the formation of the excess Si is another characteristic feature of the SIMOX BOX's, the most plausible candidate for the 2–3-eV PL center is the excess Si in the BOX. As discussed below, the similar PL from thermal oxide implanted with Si supports this assignment. The excess Si has been observed in the SIMOX BOX's in various forms from

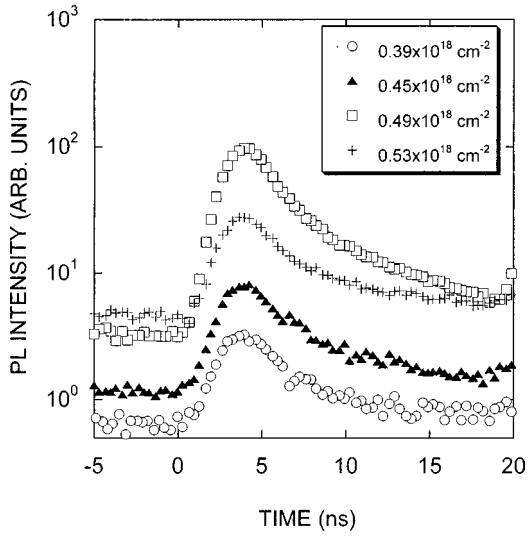

FIG. 8. The PL decay curves of the short-lived 2–3-eV PL bands obtained for the low-dose SIMOX BOX's, prepared with various oxygen doses.

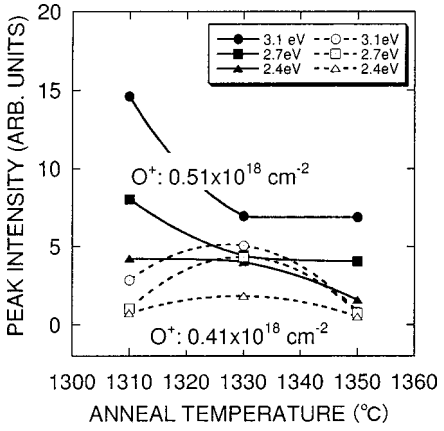

FIG. 9. Intensities of the PL bands observed for low-dose BOX as a function of anneal temperatures. Lines are drawn as a guide to the eye. ○, 3.1 eV; □, 2.7 eV; △, 2.4 eV for the dose of $0.51\times10^{18}\,\mathrm{cm}^{-2}$. ●, 3.1 eV, ■, 2.7 eV; ▲, 2.4 eV for the dose of $0.41\times10^{18}\,\mathrm{cm}^{-2}$. The 3.1- and 2.7-eV PL bands are short-lived components with lifetimes of about 2–45 ns.

crystalline platelets to amorphous Si clusters.[1] Infrared (IR) absorption measurements show the presence of excess Si in the form of $SiSi_3O$ groups in single-implant SIMOX BOX's, but not in triple-implant BOX's.[5] The observation of the increased 2–3-eV PL intensity with decreasing implant steps shown in Figs. 2 and 7 supports the idea that the 2–3-eV band is due to excess Si.

Two studies have proposed alternative mechanisms for the formation of excess-Si point defects. In both, $Si/SiO_2/Si$ structures are annealed at temperatures up to about 1300 °C and are subsequently irradiated by x or γ rays. The first is based on ESR and Fourier-transform IR studies and attributes the defect formation to oxygen from the BOX being gettered in the Si.[17] In the second, the formation of electron traps was investigated and attributed to the diffusion of a reducing species from the Si/SiO_2 interfaces into the BOX.[18]

These mechanisms may form the small Si clusters proposed as the defects responsible for the 2–3-eV PL band. As already seen for the high-temperature oxide, the formation of the 2–3-eV PL band in the SIMOX BOX's is attributed to the postimplantation, high-temperature annealing above 1300 °C. Therefore, it is concluded that the 2–3-eV PL band is associated with the formation of excess Si in the BOX as a result of oxygen gettering and/or oxide reduction during the high-temperature annealing above 1300 °C. Since the intensity of the 2–3-eV band observed for the high-temperature oxide is comparable to those of the low-dose SIMOX as shown in Figs. 4(a) and 4(b), the formation of 2–3-eV PL centers is not inherent to the SIMOX process, but it is to Si/SiO_2 interface under the high-temperature anneal.

Electrical measurements showed that SIMOX BOX's contain a higher concentration of traps when compared with conventional thermal oxide.[1–3] The traps characteristics to the SIMOX BOX's are reported to be photoactive traps, which are not observed in conventional thermal oxide.[19] The photoactive defects correlate with Si clusters in the BOX. Especially, the traps with large cross sections and large optical depth are reported to be located near the Si/BOX interface. This is consistent with the localization of the short-lived 2–3-eV PL centers in the Si/BOX interfaces, as shown in Fig. 10. The photoactive traps are dominant in SI BOX, while their density is low in TI BOX. Such a dependence on the number of implant steps quite resembles those of the 2–3-eV bands. This viewpoint is further strengthened by the results that the photoactive traps cannot be effectively removed by supplemental implant,[19] as we observed in Fig. 1. Based on these observations, it is concluded that the 2–3-eV PL centers are correlated with the photoactive deep traps in the SIMOX BOX's.

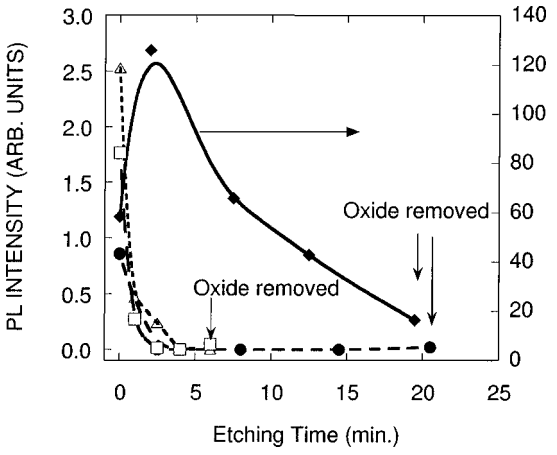

FIG. 10. The PL intensity of the 4.4-eV (◆: high-dose TI SIMOX, $1.8\times10^{18}\,\mathrm{cm}^{-2}$, 1310 °C, $t_{ox}=355$ nm) and the short-lived 2–3-eV (□: low-dose SIMOX, $0.49\times10^{18}\,\mathrm{cm}^{-2}$, 1310 °C, $t_{ox}=110$ nm, △: $0.53\times10^{18}\,\mathrm{cm}^{-2}$; 1350 °C, $t_{ox}=109$ nm, and ●: high-dose TI+suppl. SIMOX, $1.9\times10^{18}\,\mathrm{cm}^{-2}$, 1310 °C, $t_{ox}=376$ nm) bands as a function of etching time during HF etchback. The plots at the longest etching times for each curve correspond to the data for bare Si substrates. Lines are drawn as a guide to the eye.

B. Origin and mechanism of the short-lived 2–3-eV PL

As already noted, the short-lived 2–3-eV PL bands observed in the present study are not any of those reported for defects in as-grown and damaged a-SiO_2, such as neutral ODC(II) and nonbridging oxygen hole centers, in terms of the peak energy and the lifetime.[11,12,15] Interestingly, similar PL bands were reported for Si^+-implanted thermal oxide, where Si clusters are embedded in a SiO_2 matrix.[20–23] Under excitation at 5 eV, the Si^+-implanted thermal oxide exhibits three PL bands at 3.4, 2.65, and 2.4 eV.[20] A nanosecond time-resolved study on the Si^+-implanted thermal oxide[21] showed that the blue-green light emission exhibits multiple decay components with lifetimes of 0.4, 2, and 10 ns, together with the presence of millisecond or longer lifetime components. It should be cautioned that the 0.4-ns component, if any, would not be resolved in the present measurements due to the limited time resolution. Except for the 0.4-ns component, the 2–3-eV bands in the BOX's are in good accord with those observed in the Si^+-implanted thermal oxide in terms of both the peak energies and their lifetimes. This supports the foregoing attribution of the 2–3-eV band to Si clusters, since the Si^+-implanted thermal oxide is expected to contain a high concentration of excess Si in the form of Si clusters.

As for the mechanisms of the short-lived 2–3-eV PL bands, the electronic energy levels at the site of the Si clusters surrounded by a-SiO_2, wherein interface defects should be present between the Si and the oxide, should play important roles. Despite the different conditions employed to form the BOX layers, the PL peak energies are almost constant. This rules out the simple picture of a PL mechanism involving transitions between the states due to the quantum confinement effect of nanosized Si clusters, since, if it is the case, the PL peak energies should vary with the size of the Si clusters depending on the preparation conditions. As suggested by several workers,[23,24] the charge transfer between the Si clusters and oxide defects is the most plausible candidate for the PL mechanism. In fact, the threshold of the photoionization of Si clusters at 4.3 eV corresponds well with those of the onset of the PLE spectrum in Fig. 6. Very recently, photoionization and photoneutralization studies on the SIMOX BOX showed the presence of the energy states associated with the Si clusters at 2.8 and 3.1 eV below the conduction band of SiO_2.[24] The trapping of electron at the site of Si clusters was observed under the excitation of a photon energy above 4.3 eV, which agrees well with the onset of the PL excitation shown in Fig. 6. This is also consistent with the appearance of the photoinduced PL band at 2.4 eV, as well as the 3.1 and 2.6–2.8-eV PL bands due to preexisting PL centers in the BOX. They suggest the presence of the two defects levels; the 2.8 and 3.1-eV states due to the Si clusters and the H-complexed O vacancies, respectively. This is again consistent with the existence of the different PL centers shown by the presence of the multiple PL decay components. Although they suggest that visible PL bands reported for Si clusters in SiO_2 should involve charge transfer between the excess Si and oxide defects,[24] the correlation of these states with our PL bands is still unknown.

It is interesting to discuss the dose dependence of the short-lived 2–3-eV band for the low-dose SIMOX, which shows a plateau in Fig. 7(a). In a separate experiment, amorphous (a-) Si clusters, a form of excess Si, monotonically increase up to about 5% with increasing oxygen dose for the same series of low-dose SIMOX.[25] This suggests the possibility that a nonradiative recombination process at the site of the excess Si starts dominating beyond a certain amount of excess Si, while the Si clusters, i.e., the PL centers, monotonically increase with oxygen doses. However, this can be ruled out based on the result of Fig. 8, showing that there is no significant change in the PL decay lifetime. Since the PL decay lifetime τ can be expressed as the inverse of the $k_r + k_{nr}$ (k_r is the radiative decay rate and k_{nr} the nonradiative decay rate), the increasing oxygen doses give no influence on k_{nr}. This leads us to conclude that the dose of $0.49 \times 10^{18}\,cm^{-2}$ is an oxygen dose at which the Si clusters associated with the short-lived PL are efficiently formed. The increased baseline components in Fig. 8 due to much slower decay components rather correlate with oxygen doses. The slow decay component such as the one at 2.4 eV may be ascribed to the monotonic increase of a-Si clusters mentioned above.

C. Generation mechanism of the ODC(II)

There are two types of oxygen-deficient centers (ODC's). ODC(I) and ODC(II), which are characterized by their optical absorption and PL bands. A prevailing view is that the ODC(I) defects associated with the 7.6-eV absorption band are *relaxed* neutral oxygen vacancies.[16] On the other hand, the structural origin of the ODC(II) defects characterized by the 5.0-eV absorption band and 4.4-eV PL band is still controversial, while the defects are widely regarded as a form of oxygen deficiency in a-SiO_2.[16] Since discussion on the assignment of the ODC(II) to a specific structure is beyond the scope of this paper, we just mention here that there are two candidates for the ODC(II); one is *unrelaxed* oxygen vacancy, and the other is twofold-coordinated silicon.[16]

The lack of the ODC(II) in the single-implanted SIMOX BOX's is quite interesting, which is in contrast with the observation of the ODC(II) in the multiple implant SIMOX BOX's (see Fig. 7). As already noted, the additional oxygen implant into the SiO_2 during the multiple-implant process seems to be the cause of ODC(II) generation.[12] Since the multiple-implant process involves an additional implantation step of oxygen into the BOX's, the damage into the BOX is inevitable. Our previous study shows that B^+-implanted SiO_2 films exhibit the 4.4-eV PL band due to the ODC(II), which was annealed out at 500 °C either in N_2, N_2+O_2, or vacuum for 10 min.[26] Therefore, the fact that the ODC(II) was not annealed out even after the high-temperature anneal around 1300 °C is ascribed to the confined nature of the BOX sandwiched between the two silicon layers. In fact, the 4.4-eV PL band observed for a SIMOX BOX sample persisted even after the annealing up to 800 °C for 30 min in N_2, while it disappeared under the same anneal condition without a surface Si layer.[27] As suggested by the presence of strained oxide network for the BOX,[1] the annealing of the ODC(II), which should be accompanied by the relaxation of surrounding oxide network, must be hindered by the confinement effects of the sandwiched structure. In addition, the Si clusters in the BOX are expected to act as gettering sites and inhibit the supply of oxygen to the ODC(II)'s, thereby leading to the damaged region of the BOX that remained unrecovered. As described in Sec. III D, if we assume the peak of the 4.4-eV PL profile of the etchback in Fig. 10 reflects the localization of the ODC(II) in the BOX close to the top Si/SiO_2 interface, the data of the etchback suggest that the generation of the ODC(II) is maximum in the proximity of the Si clusters. This can be understood in terms of the role of the Si clusters in the BOX as gettering sites of oxygen, as discussed above.

On the other hand, the supplemental oxygen implant effectively reduced the PL of the ODC(II) generated in the TI SIMOX BOX, while more Si clusters were induced after the supplemental implant, as shown in Fig. 1. The lower postimplantation anneal temperature of 1000 °C as well as an order of magnitude lower dose of supplemental oxygen seems to be effective in the reduction of the ODC(II) in the BOX. The generation and the suppression of the ODC(II) should be determined by the ion-implantation damage and the supply of oxygen by the supplemental implantation, respectively. The lower oxygen dose of the supplemental implant can reduce the damage into the BOX layer, leading to a lower concentration of the newly induced ODC(II)'s, while the local oxygen concentration in the BOX after the supplemental implant is expected to be still high enough to react with the ODC(II) in concentrations as high as $10^{20}\,cm^{-3}$.[8] Even if we take into account the role of Si clusters as gettering sites of

oxygen, the relatively lower concentration of the Si clusters in the TI SIMOX [see the 2–3-eV band intensities of Fig. 7(b)] seems to have no significant influence on the reaction of oxygen with ODC(II). On the other hand, the increased concentration of the Si clusters after the supplemental implant process was determined both by the temperature 1000 °C and the oxygen dose $10^{17}\,cm^{-3}$, as we have already seen in Fig. 9. Therefore, optimization of both the oxygen dose and the postimplantation anneal temperature is important to suppress the generation of ODC(II) in the BOX prepared by the multiple-implant process.

V. SUMMARY

We studied the PL from the SIMOX BOX's prepared under different conditions such as oxygen dose, implant steps, and annealing temperatures. The following conclusions were drawn from the present study.

(1) Two PL bands at 2–3 and 4.4 eV were observed in the SIMOX BOX's. The 2–3-eV band consists of three subpeaks that have short decay lifetimes of 2.3–45 ns and are dominant in the low-dose SI SIMOX. On the other hand, the 4.4-eV band was mainly observed in the DI and TI SIMOX BOX's, accompanied by the short-lived 2–3-eV band and a relatively weak, long-lived 2.7-eV band. This suggests that the multiple-implant steps induced the formation of the 4.4-eV and the long-lived 2.7-eV bands associated with neutral ODC(II).

(2)Supplemental implant of oxygen suppressed the 4.4-eV band due to ODC(II) and induced two PL bands due to Si clusters in the triple-implant SIMOX BOX.

(3) The short-lived 2–3-eV bands were also observed for the high-temperature oxide grown at 1350 °C, suggesting that the 2–3-eV PL centers grow during the postimplantation annealing process. The PL band correlates with the excess Si as a result of the postimplantation, high-temperature anneal. During the anneal, the chemical reduction of the oxide is caused by oxygen diffusing out of the BOX into the Si or by a reducing species diffusing into the BOX from the Si/SiO_2 interfaces.

(4) The short-lived 2–3-eV PL centers were localized at the surface Si/BOX interface, while the 4.4-eV PL centers were located throughout the whole BOX layers.

ACKNOWLEDGMENTS

This work was performed under a Joint Study Program at IBM T. J. Watson Research Center. One of the authors (H. N.) acknowledges support from The Telecommunication Advancement Foundation during the stay in the U.S. The PL measurements were carried out using beamline U9B at the NSLS of the BNL. The authors also appreciate support from Dr. John C. Sutherland and John Trunk (BNL). We also thank Dr. Patrick J. McMarr for help with sample preparation.

[1] A. G. Revesz and H. L. Hughes, Microelectron. Eng. **36**, 343 (1997).
[2] H. E. Boesch, Jr., T. L. Taylor, L. R. Hite, and W. E. Beiley, IEEE Trans. Nucl. Sci. **NS-37**, 1982 (1990).
[3] R. E. Stahlbush, G. J. Campisi, J. B. Mckitterick, W. P. Maszara, P. Roitman, and G. A. Brown, IEEE Trans. Nucl. Sci. **NS-39**, 2086 (1992).
[4] J. F. Conley, P. M. Lenahan, and P. Roitman, IEEE Trans. Nucl. Sci. **NS-38**, 1247 (1991).
[5] I. P. Lisovskii, A. G. Revesz, and H. L. Hughes, Proc. Electrochem. Soc. **96-3**, 133 (1996).
[6] V. V. Afanas'ev, A. Stesmans, A. G. Revesz, and H. L. Hughes, J. Appl. Phys. **82**, 2184 (1997).
[7] K. S. Seol, A. Ieki, Y. Ohki, H. Nishikawa, and M. Tachimori, J. Appl. Phys. **79**, 412 (1996).
[8] K. S. Seol, T. Futami, and Y. Ohki, J. Appl. Phys. **83**, 2357 (1998).
[9] R. E. Stahlbush, IEEE Trans. Nucl. Sci. **NS-43**, 2627 (1996).
[10] J. K. Rudra and W. B. Fowler, Phys. Rev. B **35**, 8223 (1987).
[11] H. Nishikawa, E. Watanabe, D. Ito, and Y. Ohki, Phys. Rev. Lett. **72**, 2101 (1994).
[12] H. Nishikawa, E. Watanabe, D. Ito, M. Takiyama, A. Ieki, and Y. Ohki, J. Appl. Phys. **78**, 842 (1995).
[13] L. A. Kelly, J. G. Trunk, K. Polewski, and J. C. Sutherland, Rev. Sci. Instrum. **66**, 1496 (1995).
[14] R. E. Stahlbush, H. L. Hughes, and W. A. Krull, IEEE Trans. Nucl. Sci. **NS-40**, 1740 (1993).
[15] H. Nishikawa, T. Shiroyama, R. Nakamura, Y. Ohki, K. Nagasawa, and Y. Hama, Phys. Rev. B **45**, 586 (1992).
[16] L. Skuja, J. Non-Cryst. Solids **239**, 16 (1998).
[17] R. A. B. Devine, W. L. Warren, J. B. Xu, I. H. Wilson, P. Paillet, and J.-L. Leray, J. Appl. Phys. **77**, 175 (1995).
[18] R. E. Stahlbush and G. A. Brown, IEEE Trans. Nucl. Sci. **NS-42**, 1708 (1995).
[19] V. V. Afanas'ev, A. G. Revesz, and H. L. Hughes, J. Electrochem. Soc. **143**, 695 (1996).
[20] L. S. Liao, X. M. Bao, X. Q. Zheng, N. S. Li, and N. B. Min, Appl. Phys. Lett. **68**, 850 (1996).
[21] A. Pifferi, P. Taroni, A. Torricelli, G. Valentini, P. Mutti, G. Ghislotti, and L. Zanghieri, Appl. Phys. Lett. **70**, 348 (1997).
[22] H. Z. Song and X. M. Bao, Phys. Rev. B **55**, 6988 (1997).
[23] A. Kux, D. Kovalev, and F. Koch, Appl. Phys. Lett. **66**, 49 (1995).
[24] V. V. Afanas'ev and A. Stesmans, Phys. Rev. B **59**, 2025 (1999).
[25] P. J. McMarr, B. J. Mrstik, M. E. Twigg, H. L. Hughes, M. J. Anc, P. Roitman, and G. A. Garcia, GOMAC Digest **22**, 314 (1997).
[26] K. S. Seol, T. Karasawa, Y. Ohki, H. Nishikawa, and M. Takiyama, Microelectron. Eng. **36**, 193 (1997).
[27] H. Nishikawa (unpublished).